

COMPARISON OF NON-DESTRUCTIVE TESTING DEVICES TO DETERMINE IN SITU PROPERTIES OF ASPHALT CONCRETE PAVEMENT LAYERS

By

Athar Saeed, Ph.D., P.E. (Corresponding Author)

Senior Pavement Engineer
ERES Consultants Division of
Applied Research Associates, Inc.
112 Monument Place
Vicksburg, MS 39180
Phone: (601) 638-5401
Fax: (601) 634-0631
asaeed@ara.com

Jim W. Hall, Jr., P.E., Ph.D.

Director of Pavement Engineering
ERES Consultants Division of
Applied Research Associates, Inc.
112 Monument Place
Vicksburg, MS 39180
Phone: (601) 638-5401
Fax: (601) 634-0631
jhall@ara.com

Word Count: 7445

Paper submitted for presentation and publication at the
Pavement Evaluation 2002 Conference
Roanoke, Virginia

ABSTRACT

Many highway agencies use non-destructive testing (NDT) techniques for pavement evaluation. These include the falling weight deflectometer (FWD), the road-rater, the Dynaflect, the seismic pavement analyzer (SPA), the portable SPA (PSPA), the ground penetrating radar (GPR), and the dynamic cone penetrometer (DCP). Experience has shown that these techniques may not provide an accurate characterization of the in situ material properties of AC pavement layers. NCHRP sponsored research to identify and develop methods for determining the in situ modulus and thickness of asphalt concrete (AC) pavement layers and resurfacing of Portland cement concrete (PCC) pavements that improve the reliability of NDT techniques.

NDT data were collected using the FWD, SPA, PSPA, GPR and DCP at ten test sites (selected to represent typical pavement sections) in the winter and summer seasons. Data from the field tests were processed according to established methodologies. Cores from these sites were obtained for laboratory testing to determine certain physical and mechanical response parameters for use in data interpretation.

Laboratory tests were conducted to reconcile stiffness measured by field techniques to a temperature and rate of loading characteristic of vehicular traffic. The laboratory tests included the ultrasonic wave velocity method, mechanical tests (resilient modulus and the uniaxial frequency sweep), and mixture property tests.

Considering the state-of-the-practice of all the NDT technologies evaluated, the FWD and GPR were the best combination to effectively measure the AC modulus and thickness of thick AC over granular base. The SPA/PSPA also provided AC moduli that compared well with FWD moduli.

DISCLAIMER

The opinions and conclusions expressed or implied in this paper are those of authors and not necessarily those of the Transportation Research Board, the National Research Council, the Federal Highway Administration, the American Association of State Highway and Transportation Officials, or the individual states participating in the National Cooperative Highway Research Program.

RESEARCH BACKGROUND

Pavement structural evaluations are performed to predict remaining life, to allocate or restrict usage, and to plan maintenance and rehabilitation alternatives. In years past, pavement evaluations were made using empirical relationships combined with destructive testing to estimate allowable load and/or remaining life. More recently these destructive methods have been largely replaced by NDT methods. Most NDT equipment can be classified into two broad classes: 1) surface deflection-based methods, and 2) seismic or wave propagation methods. Surface deflection based methods include the Dynaflect, a number of models of the Road-Rater, and FWD devices. The Dynaflect and Road-Rater, both of which use vibratory loads, have generally been replaced with the FWD by most states. Seismic methods generate a stress wave at one point on the pavement surface and measure the time required for the waves to propagate to other points on the pavement surface. Five commonly used seismic techniques include the impact echo (IE), ultrasonic body waves (UBW), ultrasonic surface waves (USW), spectral analysis of surface waves (SASW) and impulse response (IR).

Experience has shown that these techniques may not provide an accurate characterization of the in situ material properties of the AC pavement layers due to thermo-viscoelastic nature of AC and other factors. This research evaluated NDT technique (FWD, SPA, PSPA) and ancillary devices (DCP, GRP) to determine the best combination to effectively measure AC stiffness and thickness.

RESEARCH APPROACH

NDT data were collected using the FWD, SPA, PSPA, GPR, and DCP at ten test sites (selected to represent typical pavement sections in the US) in the winter and summer seasons. Data from the field tests were processed according to established methodologies. Cores from these test sections were obtained for laboratory testing to determine certain physical and mechanical response parameters for use in data interpretation and validation.

Laboratory tests were conducted to reconcile stiffness measured by field techniques to a temperature and rate of loading characteristic of vehicular traffic. The laboratory tests included the ultrasonic wave velocity (UWV) method, mechanical tests (resilient modulus and the uniaxial frequency sweep), and mixture property tests.

FIELD TESTING PROGRAM

The field-testing plan called for in situ tests using NDT devices for new and aged, thick and thin AC and AC overlay on PCC during summer and winter months. Discussion of field-testing, data collection procedures and raw data is beyond the scope of this paper; these are discussed elsewhere¹. This paper concentrates on briefly describing the processed data and comparing the results obtained using different technologies.

NDT tests were conducted at test sites shown in TABLE 1. Five sites had a thin (≤ 125 mm) AC surface while five were categorized as thick (> 125 mm). Seven sites were categorized as flexible pavements; remaining three were composite. Three of the flexible sections contained asphalt treated base (ATB), and four contained granular base. One site was full depth AC over subgrade.

TABLE 1 Selected Details From The Field Test Sites.

Test Site	State	Location	Highway	Site Name	Construction Type	As Constructed Thickness, inch			Base/Sub-base Type
						AC	PCC	Base	
TS-1	MN	MN/Road	IH 94	Cell 17	AC	7.9	--	28	Granular/--
TS-2	MN	MN/Road	IH 94	Cell 25	AC	5.2	--	--	--
TS-3	MN	MN/Road	IH 94	Cell 29	AC	5.1	--	10	Granular/--
TS-4	MN	Scott County	US 169	LTPP 27-7090	AC/JCP	3.0	8	2	Sand/Sand
TS-5	NC	Asheville	US 25	R. Kim Site	AC	7.0	--	12	Aggregate/--
TS-6	NC	Asheville	IH 26	--	AC/JCP	2.5	9	4	Aggregate/--
TS-7	NC	Hendersonville	IH 26	--	AC/Crack/Seat	9.0	9	4	Aggregate/--
TS-8	OH	Ohio Test Road	US 23	Section S7 ¹	AC	4.03	--	10.93	ATB/Aggregate
TS-9	OH	Ohio Test Road	US 23	Section J4 ¹	AC	6.97	--	11.75	ATB/--
TS-10	OH	Ohio Test Road	US 23	Section J5 ¹	AC	7.0 ²	--	4.0 ²	ATB/Aggregate ³

Note: 1. SHRP LTPP test sections; S7: LTPP 39-0160, J4: LTPP 39-0104, J5: LTPP 39-0164

2. As designed layer thicknesses

3. Geogrid installed between aggregate subbase and subgrade

At each site, the following data were collected during field tests:

- Visual distress survey
- Deflection basins from FWD
- Seismic tests with SPA and PSPA
- Layer thickness from GPR (winter season only)
- Dynamic Cone Penetrometer testing
- Temperature of the AC layers
- Core samples for thickness and laboratory tests

All test section were 150 m in length. Data were collected at 15 m intervals in the test section and 15 m beyond and in advance of the test section in the driving lane. Tests were conducted “within” the outer wheel path and “between” the two wheel paths.

A visual distress survey was conducted in accordance with ASTM D5340² to assess existing pavement conditions prior to NDT. Each test site was divided into two sample units of approximately 280 m². Distress types, quantities and severity levels were noted for each sample unit. All test sections were in reasonably good condition.

DATA ANALYSIS AND INTERPRETATION OF RESULTS

The project objective was to identify the best combination of technologies that could effectively measure AC stiffness and thickness. To achieve this, in situ AC moduli were estimated using deflection based (FWD) and seismic based (SPA, PSPA) methods and compared.

Determination of Layer Thicknesses

Thickness of various pavement layers was determined using the GPR, DCP, SPA, and PSPA. This research used an air-coupled horn antenna GPR operating at 1 GHz suspended above the pavement surface generating 50 scans per second. TABLE 2 shows the thickness of AC pavement layer determined using GPR data, which were very close to those provided by state DOT. GPR worked best in case of AC over a granular base or PCC and had trouble distinguishing between AC and bituminous stabilized bases.

TABLE 2 Comparison Of AC Layer Thickness Determined Using Different Methods.

Test Site	AC Layer Thickness Determined Using Different Methods, mm										
	As Const.	Core	GPR	IE	SASW	IE	SASW	IE	SASW	IE	SASW
				Summer		Winter		Summer		Winter	
				Within wheel path				Between wheel paths			
TS-1	201	206 (6)	208 (8)	222 (30)	186 (8)	197 (7)	198 (11)	217 (9)	186 (8)	193 (11)	187 (13)
TS-2	132	130 (7)	130 (7)	^c	96 (4)	^c	119 (5)	^c	97	^c	118 (7)
TS-3	130	129 (9)	129 (9)	^c	105 (4)	120 (4)	124 (6)	^c	102	126 (5)	124 (10)
TS-4	76	129 (15)	125 (9)	330 ^b (36)	^c	325 ^b (34)	^c	344 ^b (45)	^c	356 ^b (51)	^c
TS-5	178	184 (7)	192 (12)	209 (21)	185 (12)	190 (10)	199 (10)	216 (22)	178 (12)	196 (15)	187 (26)
TS-6A	64	306 (13)	77 (16)	^c	^c	^c	^c	^c	^c	^c	^c
TS-6	64	74 (3)	61 (5)	312 ^b (118)	^c	263 ^b (26)	^c	55 ^b (131)	^c	290 ^b (11)	^c
TS-7	229	233 (8)	235 (16)	218 ^b (15)	^c	229 ^b (26)	^c	227 ^b (20)	^c	213 ^b (21)	^c
TS-8	102	173 (46)	120 (10)	369 ^a (29)	140 (13)	281 (59)	134 (13)	309 ^a (44)	135 (15)	236 (31)	136 (26)
TS-9	177	238 (18)	240 (9)	284 (36)	178 (11)	284 (36)	187 (16)	282 (26)	188 (13)	281 (34)	192 (19)
TS-10	102	174 (19)	183 (24)	209 (12)	147 (8)	183 (10)	162 (9)	117 (15)	146 (8)	199 (14)	163 (8)

^a - thickness most probably corresponds to the bottom of asphalt treated base.

^b - thickness corresponds to bottom of PCC.

^c - tests not conducted.

Note: Numbers in parentheses are standard deviations

Seismic data using the IE (PSPA) method provides an estimate of the AC thickness only, and the SASW (SPA) method can determine the thickness of the AC as well as underlying base/subbase layers. The AC

thicknesses estimated using seismic data during summer were generally smaller than those in winter, but generally within 10 to 15% of the cores thicknesses. The IE method is quite suitable for concrete layers and was used for estimating asphalt thickness for the first time in this project.

Data in TABLE 2 indicate that as-constructed AC layer thicknesses were very close to those measured using cores. Test sections TS-8, -9 and -10 contained an AC layer over an asphalt treated base. The core thicknesses (interfaces) could not be established precisely for these sections; this may be the reason for the slight discrepancy between GPR and core data. SASW tests were not be interpreted for test sites TS-4, TS-6 and TS-7 because according to the developers of the SPA, the current sensor configuration of SPA does not allow for a reliable analysis of the data for this condition.

The thickness of the base layer was estimated using DCP, GPR, and SPA data (see TABLE 3). GPR did not differentiate between AC and asphalt treated base and the results had to be calibrated using AC thickness data from cores (TS-8, TS-9, and TS-10). The SPA provided the thicknesses of the granular bases as well as ATBs. However, as indicated above, the SASW thicknesses from the SPA tests are not available for pavements incorporating a PCC layer (TS-4, TS-6, TS-6A, and TS-7). DCP tests were only conducted in unbound pavement layers.

TABLE 3 Comparison Of Base Layer Thickness Determined Using Different Methods.

Test Site	Base Layer Thickness (mm)						
	State DOT Provided Information			GPR		SPA ^a	DCP ^b
	Construction Type	PCC	Base	PCC	Base	Base	Base
TS-1	AC / granular base	--	711	--	--	598	669
TS-2	AC / subgrade	--	--	--	--	276 ^c	--
TS-3	AC / granular base	--	254	325	--	262	289
TS-4	AC / JCP / sand subbase	203	51	260	--	--	302
TS-5	AC / granular base	--	305	--	--	298	313
TS-6A	AC / JCP	229	102	250	64	--	118
TS-6	AC / granular base	229		317	--	--	
TS-7	AC/Crack & Seat	229	102	240	--	--	107 ^d
TS-8	AC + asphalt treated base	--	278	--	313	271 ^d	127 ^e
TS-9	AC + asphalt treated base	--	298	--	368	310 ^d	--
TS-10	AC + asphalt treated base	--	94	--	218	109 ^d	204 ^e

^a Average of summer and winter tests and between the wheel paths and within the wheel path run

^b Average of summer and winter tests conducted at the core locations

^c TS-2 was thin AC directly over the subgrade, SPA detected a different modulus for the top and bottom [art of the layer

^d Only one location

^e Layer AC thickness

FIGURE 1 compares the base thicknesses determined using the different technologies with as-constructed thicknesses. Data for stabilized and granular layers were combined to prepare the plots. DCP and SPA data do not include bound layer information, and the data set for GPR does not include granular layer information. From the slope of the best-fit lines in FIGURE 1, the GPR estimate the base thickness with an accuracy of better than 19 percent and the SPA with an accuracy of about 10 percent.

Determination of In Situ Layer Moduli

Determination of AC Layer Moduli

In situ elastic modulus of AC layer was determined using FWD, SPA, and PSPA data.

The AC layer thicknesses determined using the GPR were used in the backcalculation procedure of the FWD deflection data. FWD backcalculated AC modulus at each of the ten sites are shown in TABLE 4. TS-6 was selected as an AC overlay of a jointed concrete pavement; however, GPR data indicated approximately 90 m of full depth AC pavement. This portion of the site was labeled as TS-6A and was as such. AC modulus-temperature relationship developed by Lukanen et al.³ was used for temperature adjustment. Adjusted moduli are shown in TABLE 4.

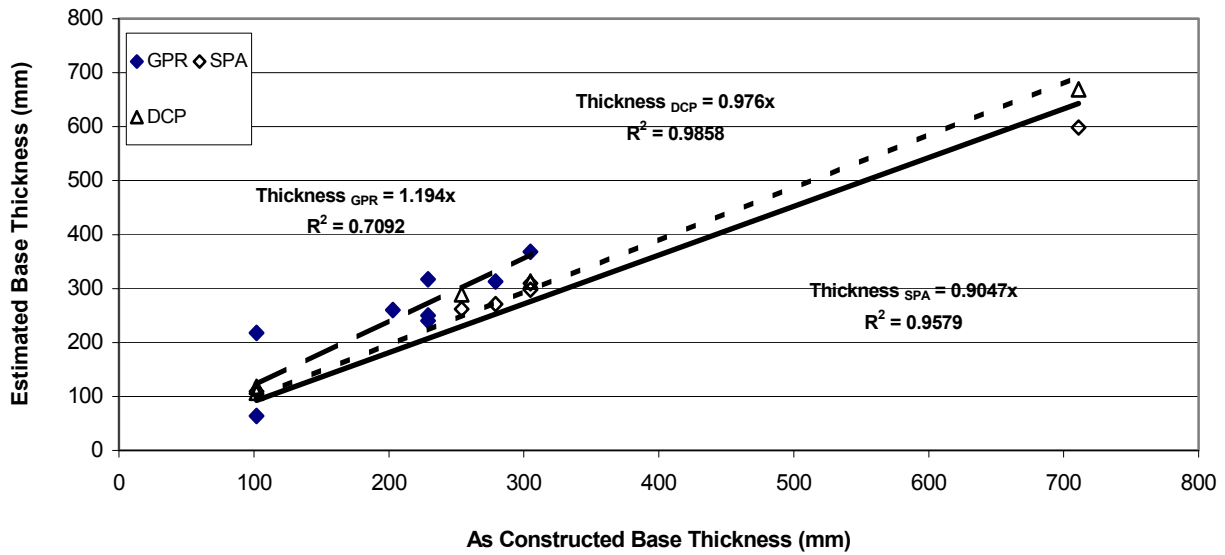


FIGURE 1 Comparison of base layer thickness from GPR, SPA, and DCP methods.

TABLE 4 FWD Backcalculated AC Modulus At Field Temperature And Adjusted To 25 °C.

Test site	Backcalculated Modulus (Summer), GPa				Backcalculated Modulus (Winter), GPa			
	Within wheel paths		Between wheel paths		Within wheel paths		Between wheel paths	
	Modulus	Adj. 25°C	Modulus	Adj. 25°C	Modulus	Adj. 25°C	Modulus	Adj. 25°C
TS-1	2.64	2.89	3.47	3.82	8.82	3.28	11.72	4.05
TS-2	3.26	6.69	2.14	4.64	8.46	3.77	9.11	3.82
TS-3	0.78	1.34	0.89	1.59	3.61	3.16	4.74	4.10
TS-4	9.06	9.91	7.72	8.50	10.16	5.18	13.94	6.75
TS-5	2.51	3.14	3.33	4.24	10.57	4.31	9.31	3.54
TS-6A	1.88	2.95	1.55	2.51	4.68	3.27	5.05	3.43
TS-6	1.08	1.69	0.79	1.28	2.61	1.82	2.92	1.98
TS-7	3.42	4.09	3.88	4.71	12.62	6.44	13.1	6.34
TS-8	2.38	3.41	2.22	3.27	7.34	3.27	7.43	3.11
TS-9	3.34	3.49	3.28	3.44	9.07	4.04	9.16	3.84
TS-10	4.29	7.69	2.99	5.61	8.84	3.94	10.57	4.43

The PSPA data are reduced to estimate AC layer moduli using the USW method and the thickness of the AC layer using the IE method. The SPA data were used to determine the modulus and thickness of various pavement layers using the SASW method. The effective modulus of the whole pavement structure was determined using the IR method.

Table 5 lists the field and adjusted AC layer moduli using the USW and SASW methods for tests conducted within the wheel path. The moduli between the wheel paths were generally greater than moduli within the wheel path. The relationship, shown below, suggested by Li and Nazarian⁴ for adjusting the modulus of AC to a reference temperature of 25 °C was used.

$$E_{25} = E_t / (1.35 - 0.014 t) \quad (E_{25} \text{ and } E_t \text{ are moduli at } 25 \text{ and } t \text{ } ^\circ\text{C})$$

To adjust the seismic estimated AC moduli to the frequency and strain levels similar to those measured with an FWD, Aouad et al.⁵ propose that the seismic modulus at 25 °C should be divided by a factor of three. Table 5 seismic AC moduli are adjusted for both temperature and strain-rate.

TABLE 5 AC Moduli Estimated Using USW and SASW Methods.

Test Site	AC Modulus, GPa							
	Winter Testing				Summer Testing			
	PSPA USW Method		SPA SASW Method		PSPA USW Method		SPA SASW Method	
	Field	Adjusted	Field	Adjusted	Field	Adjusted	Field	Adjusted
Within the Wheel Path								
TS-1	18.87	5.30	17.60	4.95	11.62	3.98	11.80	4.08
TS-2	15.51	4.73	14.68	4.48	8.35	3.12	8.89	3.32
TS-3	14.66	4.44	14.30	4.33	7.01	2.59	9.80	3.62
TS-4	19.45	5.61	--	--	13.64	4.71	--	--
TS-5	16.75	4.77	15.63	4.45	11.52	4.01	10.93	3.81
TS-6	10.39	3.47	--	--	6.83	2.65	--	--
TS-7	14.93	4.40	--	--	11.21	3.88	--	--
TS-8	18.16	5.12	17.75	5.00	15.07	5.59	12.97	4.81
TS-9	16.73	4.63	18.51	5.12	14.24	4.84	14.28	4.85
TS-10	15.08	4.24	17.51	4.92	11.1	3.94	10.59	3.77
Between the Wheel Paths								
TS-1	20.57	5.78	17.73	4.98	12.83	4.5	11.85	4.16
TS-2	15.92	4.86	14.45	4.41	8.17	2.99	9.02	3.3
TS-3	15.61	4.73	14.27	4.32	7.39	2.72	9.7	3.57
TS-4	20.95	6.04	--	--	14.05	4.93	--	--
TS-5	18.45	5.25	16.45	4.68	12.44	4.46	10.98	3.9
TS-6	10.37	3.46	--	--	6.77	2.57	--	--
TS-7	12.44	3.66	--	--	9.89	3.26	--	--
TS-8	--	--	--	--	--	--	--	--
TS-9	15.67	4.33	18.09	5	13.74	4.53	14.21	4.68
TS-10	16.09	4.52	17.48	4.91	11.82	4.05	11.57	3.97

Comparison of SPA/PSPA and FWD AC Moduli

The modulus of the AC layer was backcalculated from the FWD deflection data. The USW method used with the PSPA data provides a direct measurement of the modulus of the AC without a need for a backcalculation. The SASW dispersion curve is used to backcalculate the velocity of the AC layer, which is converted to modulus. FIGURES 2 and 3 plot AC moduli estimated using winter and summer field data using seismic-based and deflection-based techniques for “within the wheel path” and “between the wheel paths” tests, respectively. Generally, there is good agreement between moduli determined using deflection and seismic data.

FIGURE 4 shows a fairly strong relationship between AC layer moduli from FWD and SPA and PSPA tests at field conditions; a strong relationship between adjusted backcalculated moduli from FWD and seismic methods could not be achieved due to different temperature correction relationships used. The results from concrete overlaid sites were included in the PSPA correlation.

Base Layer Modulus

The base layer modulus was determined using the FWD deflection data, SASW results from SPA testing, and DCP testing. DCP data were used to estimate the CBRs, which were then converted to modulus using the following relationship:

$$E = \text{CBR (1500)}, \text{ where } E \text{ is in psi}$$

FIGURE 5 shows that there was little difference between the base layer moduli estimated for “within the wheel path” tests and the “between the wheel paths” tests using from either the SASW method or FWD data analysis. However, the SASW moduli were consistently higher than those estimated using the FWD data. This

trend is reasonable because seismic moduli are low-strain moduli, whereas the FWD moduli are at higher strain levels. SASW analysis was not conducted for the rigid layer in test sites TS-4, TS-6, and TS-7. Base moduli determined using DCP also indicate no difference between summer and winter tests, except for TS-5.

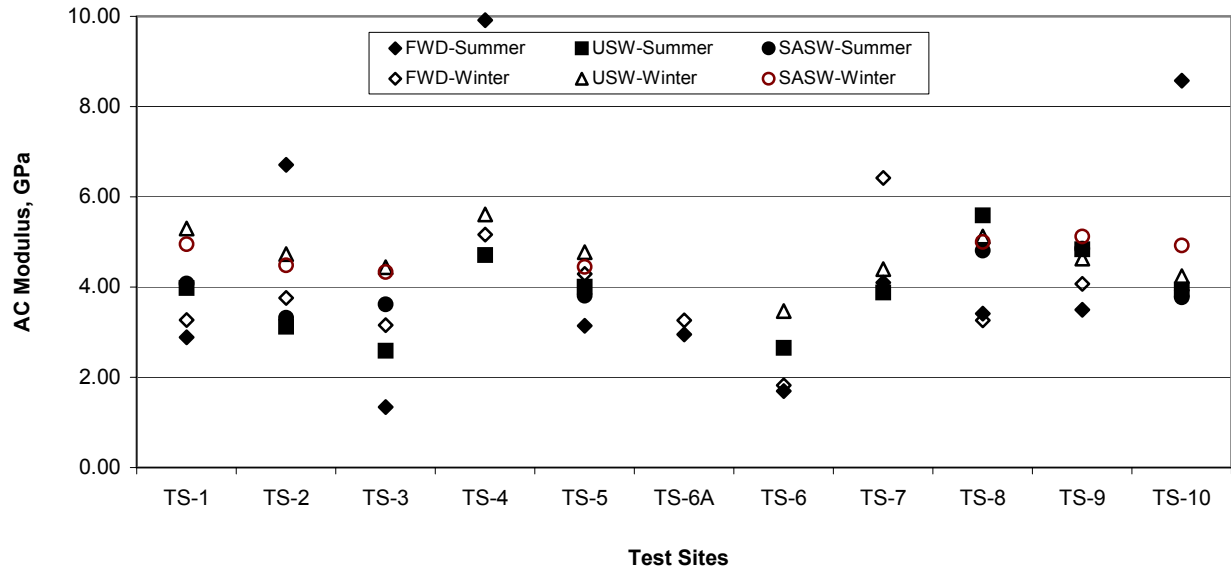


FIGURE 2 Comparison of “inside the wheel path” AC modulus.

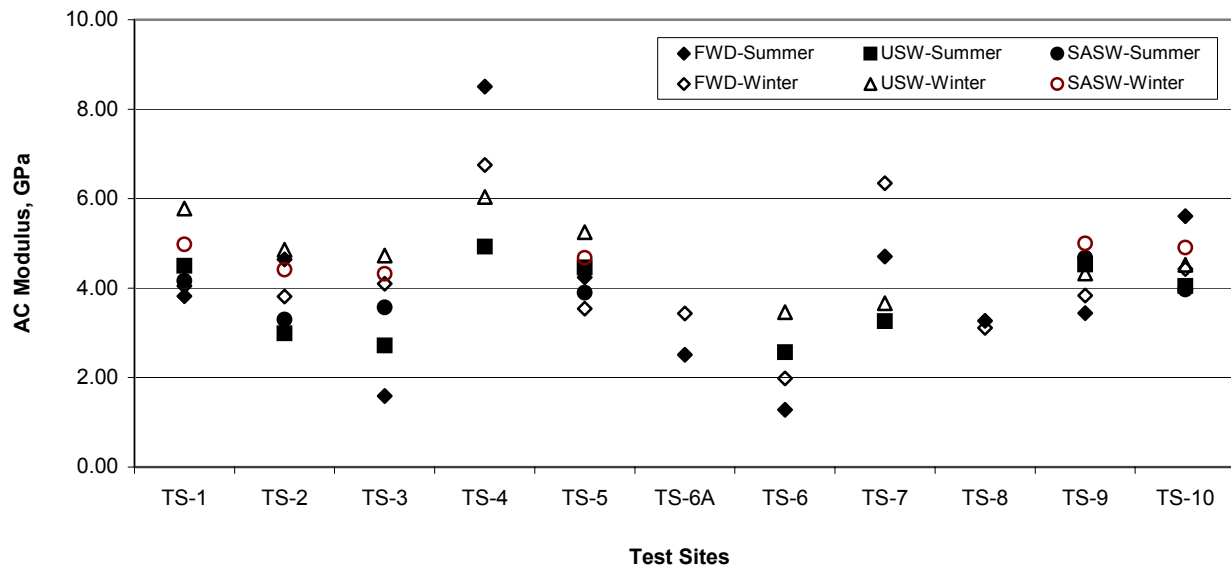


FIGURE 3 Comparison of “between the wheel paths” AC modulus.

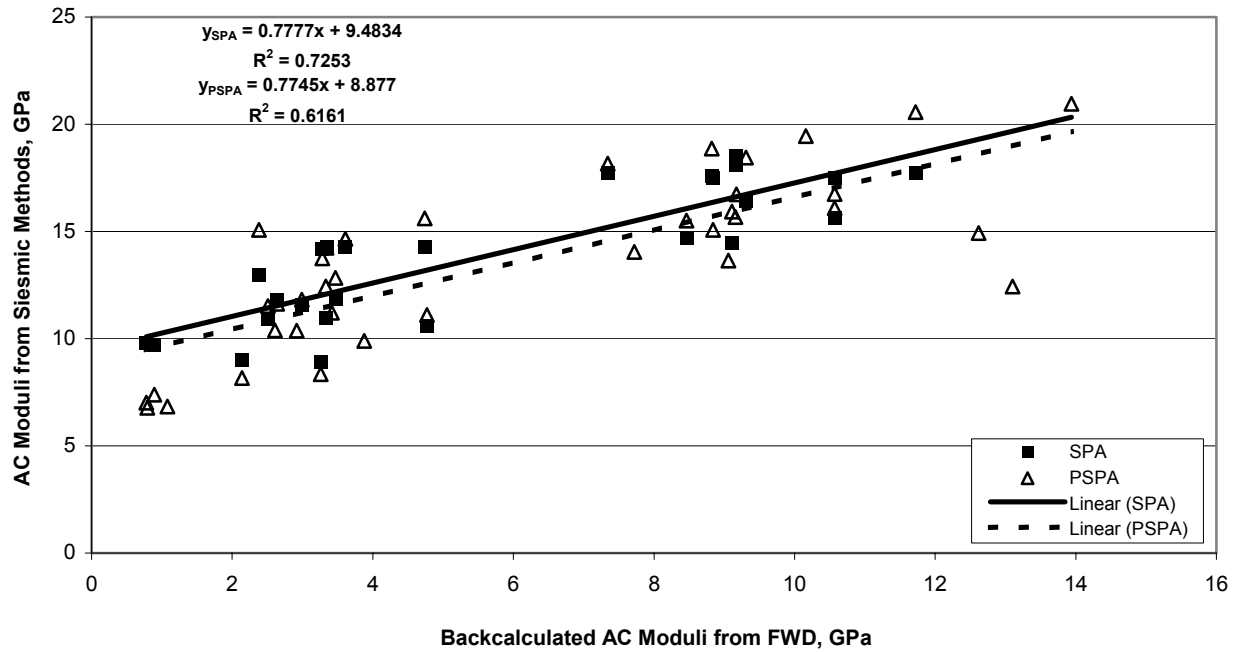


FIGURE 4 Relationship between AC moduli from FWD and seismic methods at field conditions.

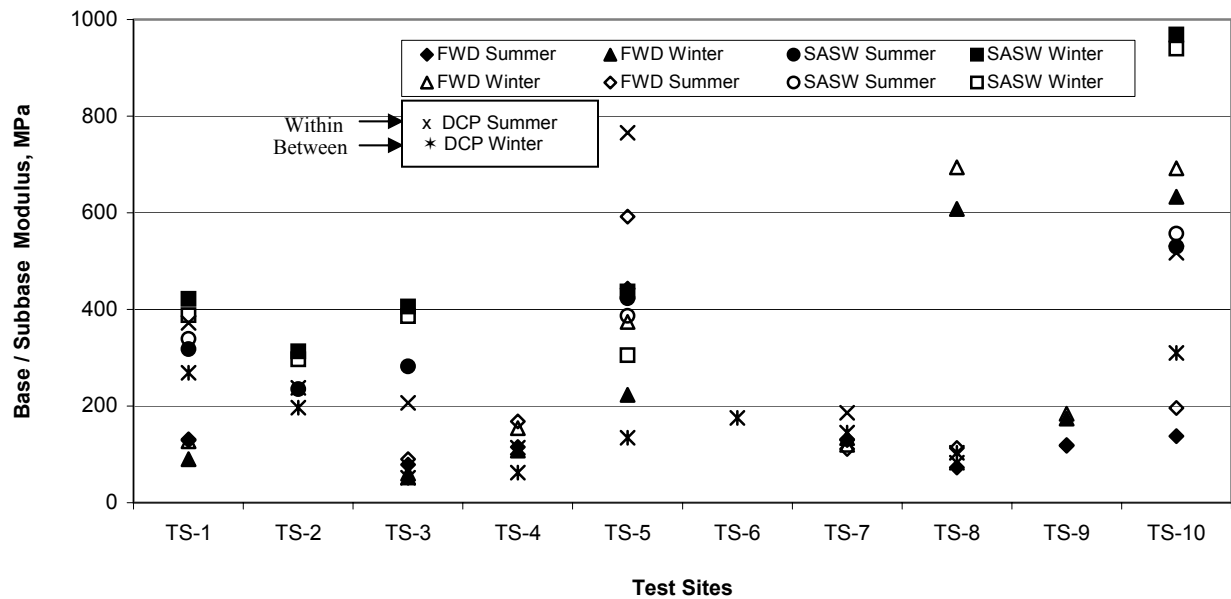


FIGURE 5 Comparison of base moduli estimated using SASW, FWD, and DCP methods.

Subgrade Modulus

The average subgrade moduli estimated using FWD, SPA and DCP data are compared in FIGURE 6. For most sites, the SPA data gave summer moduli that are slightly lower than the winter moduli. FWD backcalculated also followed the same general trend of summer moduli being lower than winter moduli. The difference in magnitude between winter and summer tests was not attributed to a frozen subgrade or other layers. The DCP-derived moduli also follow the same trend.

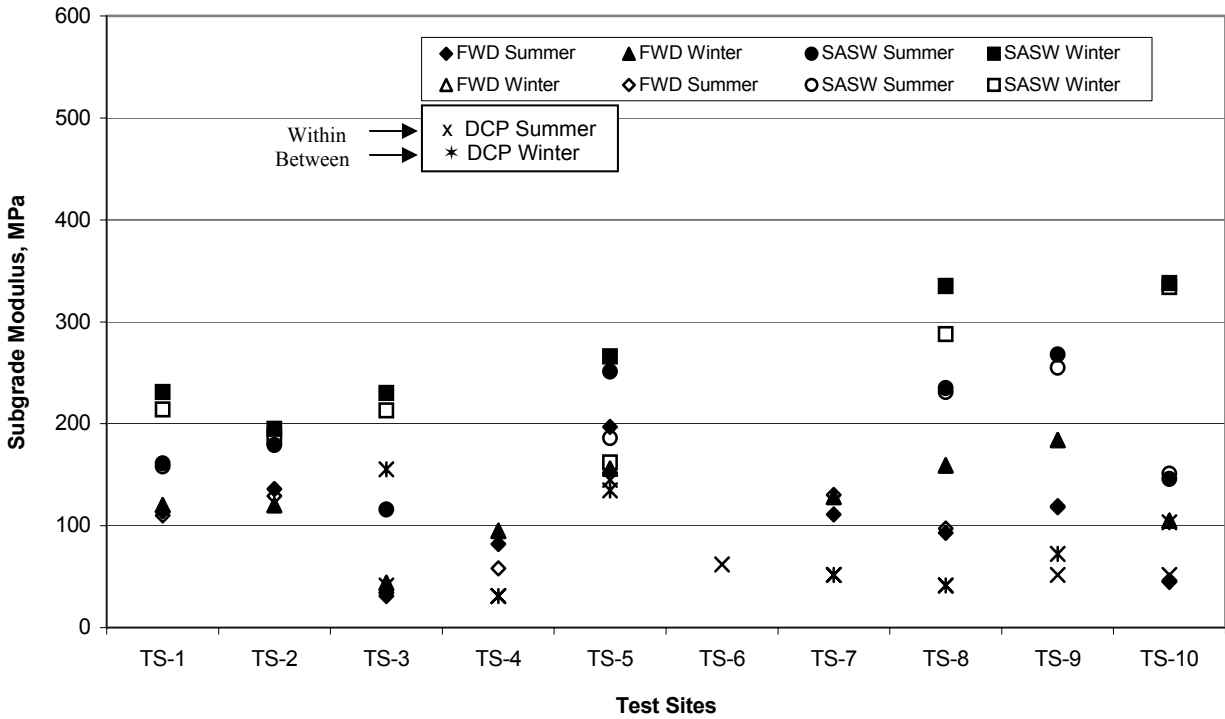


FIGURE 6 Comparison of subgrade moduli estimated using SASW and FWD deflection data.

Overall Composite Modulus

The IR method provides an overall composite modulus of the pavement structure. A reduction in the AC layer modulus tends to decrease the composite pavement modulus. The composite modulus is also sensitive to granular layers characteristics. FIGURE 7 shows a strong relationship between composite pavement modulus determined from SPA and FWD data. There was little difference between the composite modulus from “within the wheel path” and “between the wheel path” tests for the winter and summer months, therefore, these were combined to develop the plot shown in FIGURE 7.

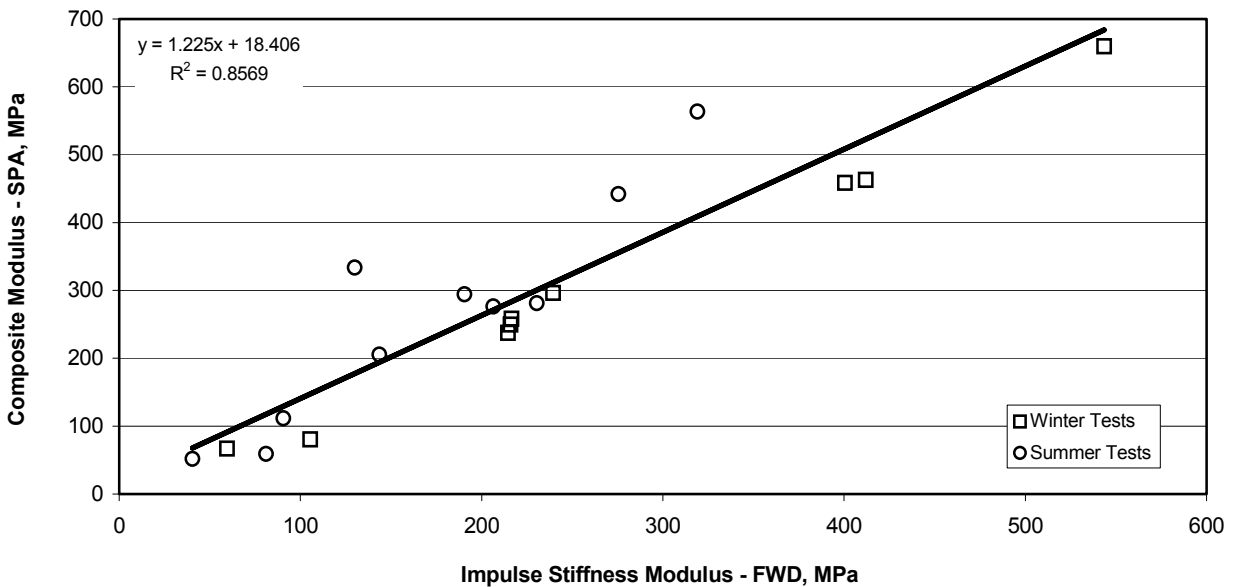


FIGURE 7 Relationship between composite modulus from FWD and SPA at field conditions.

LABORATORY TESTING PROGRAM

The laboratory test program to determine the AC moduli was conducted using two different test approaches. The first approach called for determining the AC modulus using the UWV method and the second schemes used mechanical tests. The mechanical tests included the resilient modulus (M_R) test and the uniaxial frequency sweep test. Physical properties such as bulk specific gravities, AC content, air voids, and extracted aggregate gradation were also determined.

The UWV method determined the elastic modulus of the specimen. FIGURE 8 plots the adjusted moduli and the standard deviation ranges. TS-6 exhibits a relatively large standard deviation because two cores out of the six were very thin. Saeed and Hall¹ show that the seismic moduli from the UWV were within 20 percent of those from the PSPA and SPA.

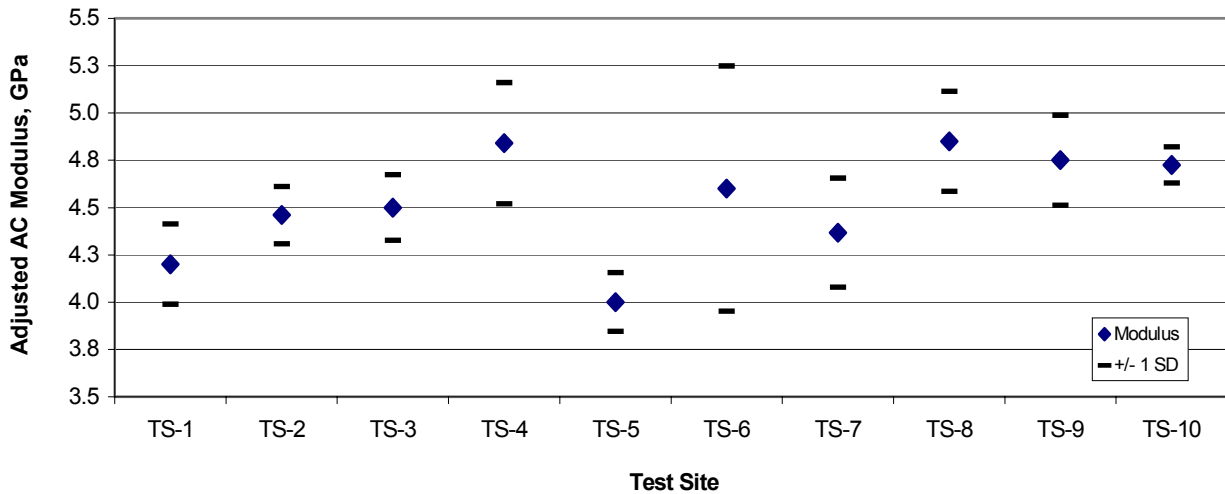


FIGURE 8 Average adjusted AC modulus using ultrasonic wave velocity method.

Diametral M_R tests (ASTM D4123) were conducted at 25 °C on AC cores prior to conducting the frequency sweep tests. Cores from site TS-6 could not be tested. Data did not indicate a significant difference between M_R values from between wheel paths and within wheel path.

Shear frequency sweep tests at constant height (AASHTO TP7-94, Procedure E) were conducted at -17, 4, 40 and 60 °C and at test frequencies of 0.1, 1, 10 and 25 Hz (not same as AASHTO TP7-94 specified frequencies). The 25-Hz frequency was selected to encompass the loading frequency of the FWD. FIGURE 9 shows the typical stiffness versus frequency plot for the four test temperatures with FWD data superimposed to illustrate that frequency sweep test data can be used to compare moduli estimated at different frequencies.

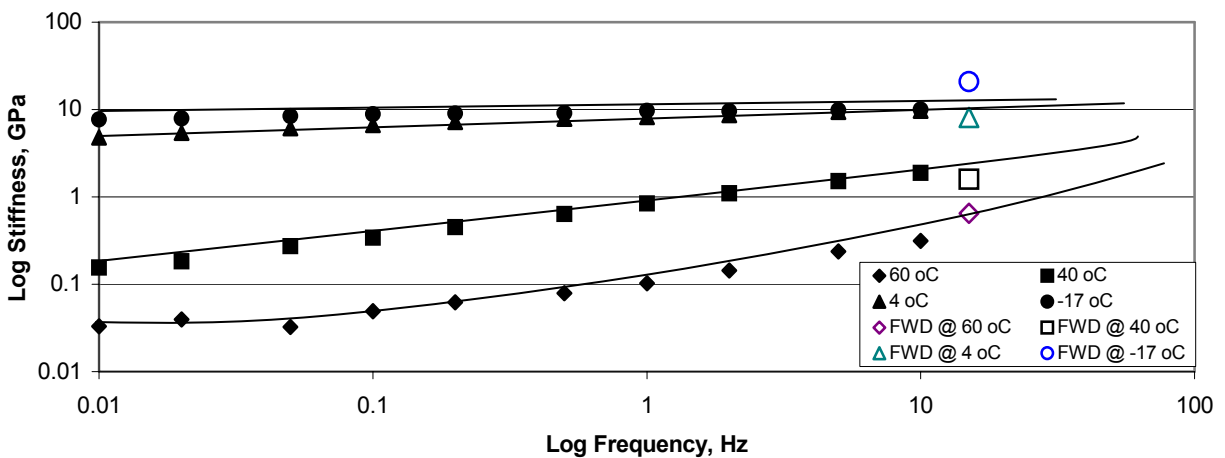


FIGURE 9 Frequency sweep test results from test site TS-5 with FWD data superimposed.

Frequency sweep data were used to develop master curves that describe the loading rate (time) dependency of modulus at a reference temperature. Master curves can be used to compare stiffness of different mixes at different temperatures and loading rate. FIGURE 10 shows a typical master curve with the FWD and seismic moduli superimposed on it. Both the FWD and seismic moduli lie reasonably close to the master curve. FWD and seismic moduli for other test sites were also reasonably close to the mater curves.

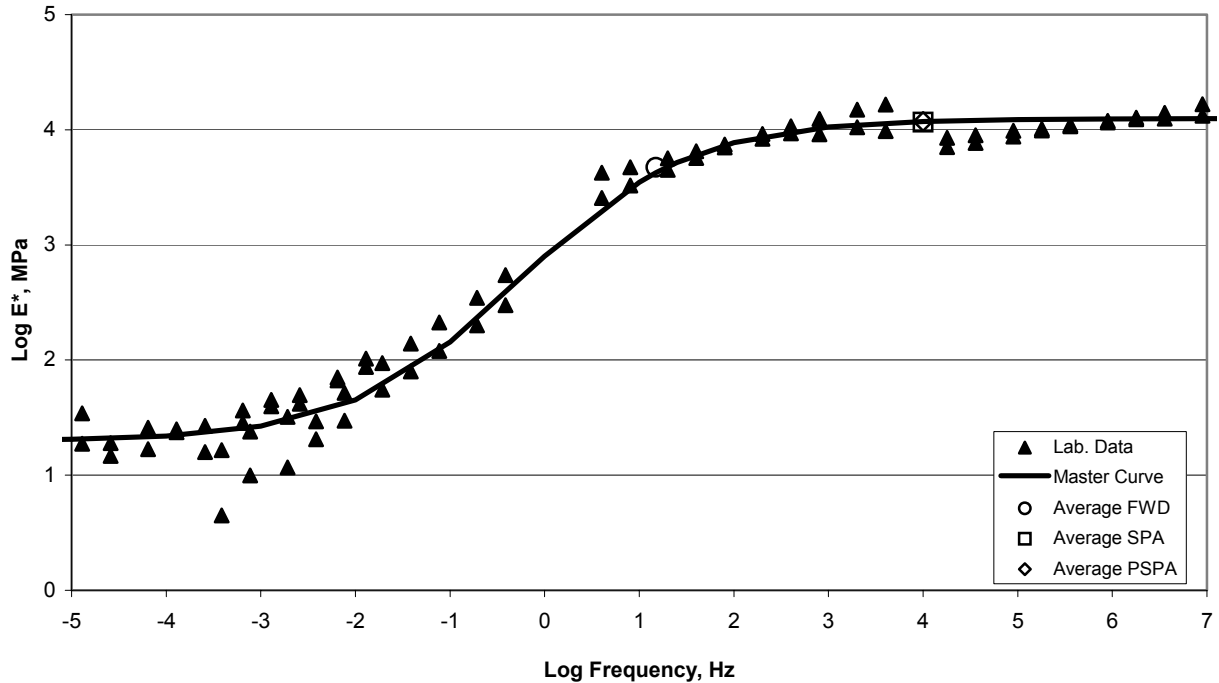


FIGURE 10 Master curve for test site TS-2 at 25 °C reference temperature.

FIGURE 11 shows dynamic moduli at 15 Hz and 25 °C for AC samples from each test site estimated using master curves. The cores from test sites TS-6 and TS-7 could not be tested. The backcalculated average FWD and seismic moduli are also plotted on FIGURE 11; there is no clear trend between laboratory dynamic modulus from master curves and the in-situ moduli from deflection and seismic methods.

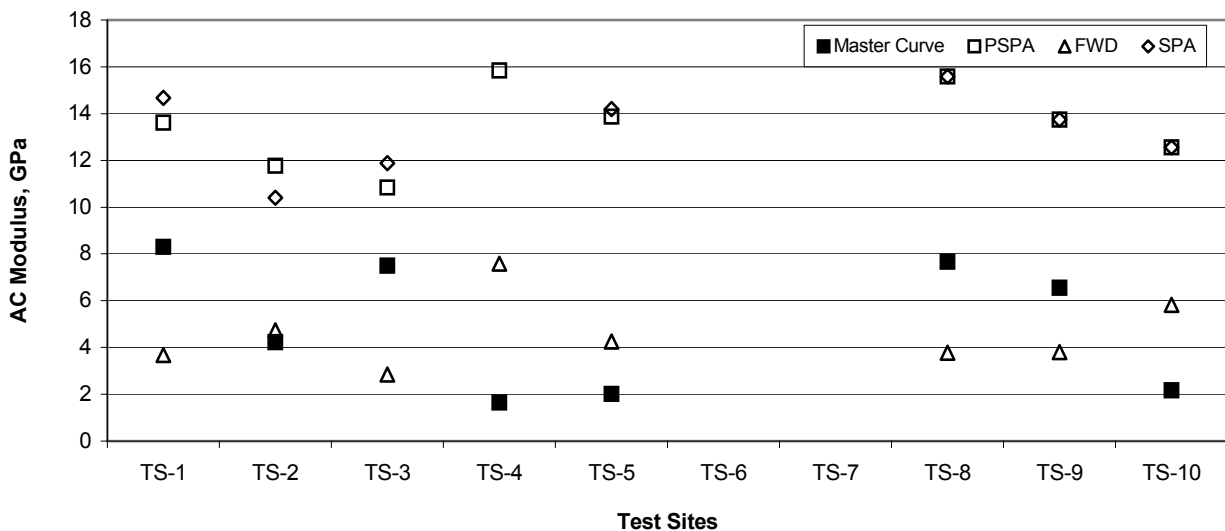


FIGURE 11 Comparison of AC modulus for the test sites.

FIGURE 12 shows a good relationship between M_R and modulus determined using seismic methods (adjusted to 25 °C); however, PSPA did not have a strong relationship with laboratory determined M_R . A reasonable relationship could not be archived between M_R and FWD backcalculated modulus.

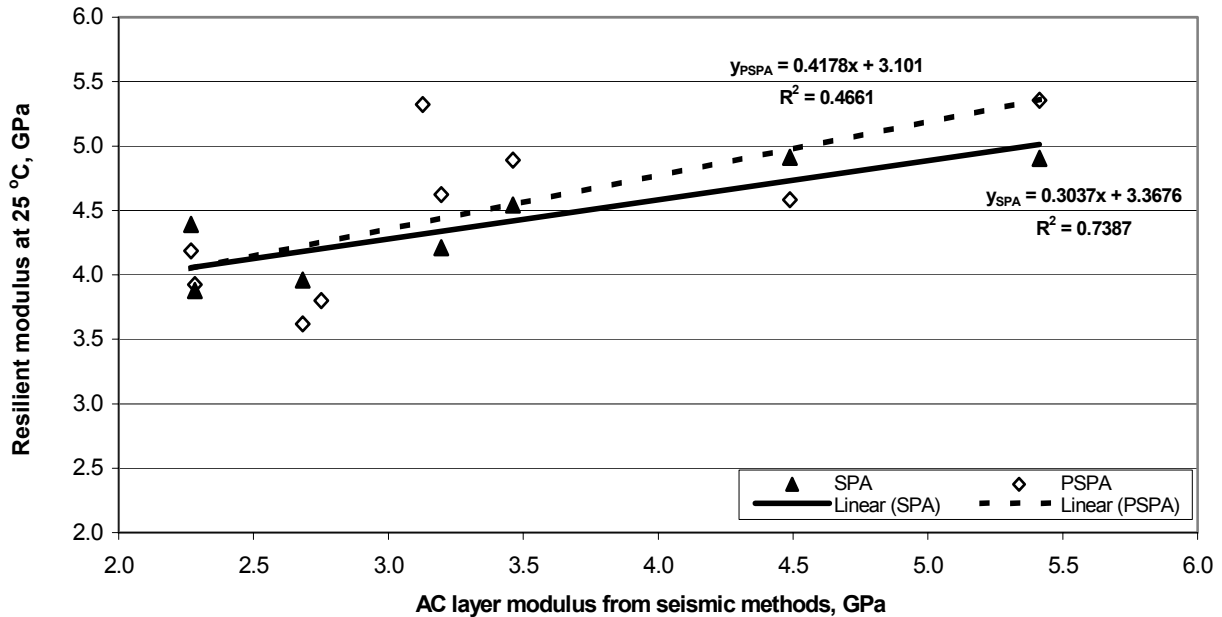


FIGURE 12 Comparison of seismic modulus with resilient modulus test results at 25 °C.

DATA ANALYSIS SUMMARY AND CONCLUSIONS

Tests were conducted during the winter and summer seasons at ten test sites located in different geographical regions of the U.S. Different combinations of deflection, seismic and laboratory-based technologies were used to estimate the in situ modulus of the AC layer.

GPR, seismic, and core data were analyzed to determine the thickness of the AC layer. Six cores were taken through the length of each test section. GPR estimated thicknesses had the best relationship with cores followed by SPA data analyzed with the SASW methodology. GPR also proved to be beneficial in determining discontinuities and structural changes in the section.

Information about pavement layer thicknesses is essential for backcalculating layer moduli from deflection data. The AC layer moduli estimated using seismic methods also showed the same trend as shown by FWD backcalculated moduli.

Seismic techniques alone have potential to measure both thickness and modulus of AC surface. The AC layer thickness measured using the SPA compared well with core thicknesses.

Based on the results of the research, the following conclusions are warranted.

1. Considering the state-of-the-practice of all the NDT technologies evaluated, the FWD and GPR were the best combination of technologies to effectively measure the AC stiffness and thickness. Note that seismic methods also gave comparable results.
2. There was a good correlation between FWD backcalculated modulus values and modulus values from seismic (SPA and PSPA) data.
3. There was good agreement between AC modulus from seismic methods and that determined from the laboratory resilient modulus test.
4. Some limitations of the SPA that require further development in order to make it suitable for routine use are: 1) it is unable to test composite pavements; 2) equipment reliability problems also hinder smooth and timely data collection.
5. GPR results agreed well with core thicknesses but the GPR could not differentiate between the AC surface layer and ATB layer.

ACKNOWLEDGEMENTS

ERES Consultants, a Division of Applied Research Associates, Inc., performed the research under NCHRP Project 10-44A.

National Center for Asphalt Technology conducted the laboratory tests. Terracon, Inc., provided FWD, GPR, and DCP testing support. Geomedia Research and Development, Inc. conducted seismic testing. Infrasense, Inc. analyzed the GPR data. Drs. Soheil Nazarian and Matt Witzak, and Mr. Tom Scullion served as consultants.

The support provided by North Carolina, Minnesota, and Ohio DOTs and NCHRP during the course of this project is also acknowledged.

REFERENCES

1. Saeed, A., and J.W. Hall, Jr. Determination of In Situ Material Properties of Asphalt Concrete Pavement Layers. Report, NCHRP 10-44, TRB, National Research Council, Washington, DC, 2001.
2. Standard Test Method for Airport Pavement Condition Index Surveys. ASTM D5340-93, ASTM, Philadelphia, 1993.
3. Lukanen, E. O., R. Stubstad, and R. Briggs. Temperature Predictions and Adjustment Factors for Asphalt Pavements. Report FHWA-RD-98-085, FHWA, U.S. Department of Transportation, 1992.
4. Li, Y., and S. Nazarian. Evaluation of Aging of Hot Mix Asphalt Using Wave Propagation Techniques. In *STP 1265*, ASTM, Philadelphia, PA, 1994.
5. Aouad, M.F, K. H. Stoke, II, and R.C. Briggs. Stiffness of Asphalt Concrete Surface Layer from Stress Wave Measurements. In *Transportation Research Record 1384*, TRB, National Research Council, Washington, DC, 1993, pp. 29 - 35.